Investigation of Structure and Magnetic Properties of Polycrystalline $La_{0.7}Ba_{0.21}Ca_{0.09}Mn_{1-x}Ni_xO_3$ (x=0.1, 0.2, 0.3) by Sol Gel Method

P. Prasetyo[1], S.A. Saptari[1*], A. Tjahjono[1] & B. Kurniawan[2]

[1] Department of Physics, Faculty of Science and Technology, UIN Syarif Hidayatullah Jakarta, Indonesia
[2] Department of Physics, University of Indonesia, Indonesia

Article Info	ABSTRACT
  Corresponding Author: S.A. Saptari, Department of Physics UIN Syarif Hidayatullah Email: sitti.ahmiatri@uinjkt.ac.id	Polycrystalline $La_{0,7}Ba_{0,21}Ca_{0,09}Mn_{1-x}Ni_xO_3$ (x = 0,1; 0,2; 0,3) have been synthesized using sol-gel method, the precursors material from pro analysis products. Samples had characterized by XRD, SEM, and VSM. The result of refinement from XRD pattern shown that all materials had single phase with the lattice parameter a and b had decreased with increasing Ni+3 ion and had a rhombohedral structure along with R-3c space group. The materials had nanoparticle distribution particle size based on measurement by SEM. Hysteresis loop shown that the samples $La_{0,7}Ba_{0,21}Ca_{0,09}Mn_{1-x}Ni_xO_3$ (x = 0,1; 0,2; 0,3) are soft magnetic material. Moreover, the increase of Ni^{+3} ion gave an impact about the magnetization decreasing from the materials which shown by the decreasing of magnetic saturation value. *Keyword: : $La_{0,7}Ba_{0,21}Ca_{0,09}Mn_{1-x}Ni_xO_3$, magnetic saturation value*

1. INTRODUCTION

Lanthanum manganese has general formula $Re_{1-x}A_xMn_{1-y}B_yO_3$ with Re is Lanthanum ion (La^{+3}), A is divalent alkali ion, and B is transition metallic ion (Millis, 1998; Nagabhushana, et al, 2008). The structure is from first perovskite structure ABO_3. Because of the good stability of a perovskite structure, then the perovskite structure can be doped at the site A with trivalent rare earth ion and/or divalent alkali ion, besides at the site B can be doped by transition ion metallic (Stege, Cadús and Barbero, 2011; McBride, et al, 2017; Bhavani, Kim & Lee, 2013).

Differences of substitution on the lanthanum manganese are influential for structure, spin condition, and electron transport than others influence. Therefore, lanthanum manganese has been studied (McBride, et al, 2017; Zhong, et al, 2003; Xiong, et al, 2015). Lanthanum manganese is very interesting in science and technology field, where the lanthanum manganese can be applied for magnetic refrigeration, magnetic switches, magnetic sensor (Nagabhushana, et al, 2008; Phan, et al, 2007), microwave absorber (Jiang, et al, 2015), electrode supercapacitor (Cao, et al, 2015) and data storage (Saptari, et al, 2017).

Recently, the studied of structure and magnetic properties of lanthanum manganese with doping shown a change magnetization and the structure which does not change significantly (McBride, et al, 2017; Saptari, et al, 2017; Manjunatha, et al, 2015; Sfifir, et al, 2017). In the studied from Mc Bride et al (2017), known that the lanthanum manganese with barium ion (Ba^{+2}) doped on A site has currie temperature at 312 K. However the doped calcium ion (Ca^{+2}), lanthanum manganese has currie temperature at 262 K, with the saturation value is higher than barium doped. If the lanthanum

manganese has doped by calcium and barium ion, the temperature currie would reach 302 K (Sfifir, et al, 2017).

In this studied we use calcium and barium ion for doping lanthanum ion and nickel ion (Ni^{+3}) for doping manganese ion (Mn^{+3}). Because of the rare earth ion doped by divalent ion, then the Mn^{+3} ion changed into Mn^{+4} ion, it called double exchange relation (Mn^{+3}-O^{-2}-Mn^{+4}) (Nagabhushana, et al, 2008; Morelli, et al, 1996).

The material has fabricated by the sol-gel method. Sol-gel method has many advantages, two of them produce a homogeneous particle with nanoparticle size and efficiency used for energy due to sintering if compare with solid state method (Nagabhushana, et al, 2008; Shankar & Raychaudhuri, 2006). In this work we observed the effect Ni of doped on the structure, morphology, and magnetization from polycrystalline $La_{0.7}Ba_{0.21}Ca_{0.09}Mn_{1-x}Ni_xO_3$ (x = 0.1; 0.2; 0.3) which can be applied to microwave absorber (Saptari, Manaf & Kurniawan, 2014).

2. RESEARCH METHOD

$La_{0.7}Ba_{0.21}Ca_{0.09}Mn_{1-x}Ni_xO_3$ (x = 0.1; 0.2; 0.3) were fabricated using sol-gel method with precursors of samples are $C_6H_8O_7$ H_2O (Merck, 99.5%), $Ni(NO_3)_2$ .6 H_2O (Merck, 99.0 %), $Ca(NO_3)_2$ .4H_2O (Merck, 99.0 %), $Mn(NO_3)_2$ .4 H_2O (Merck, 98.5 %), La_2O_3 (Merck, 99.0%), and $Ba(NO_3)_2$ (Merck, 99.0 %). Each of precursors have calculated by stoichiometry formula. Nevertheless, for La_2O_3, it has added nitrate acid based on stoichiometry calculation, to convert carbonate became nitrate.

Then, all precursors dissolved with aquabidest, and mixed all precursors into one solution. The solution was heated and added with ammonium solution until pH reached the value of 7 at 343-353 K. After that, the gel was heated at the temperature of 423 K during 4 hours until the gel dried. Afterward, the gel had calcinated at 873 K for 8 hours. Finally, the gel has been sintering at 1123 K for 10 hours.

The structure has characterized by X-Ray Diffraction with the Cu-Kα radiation to determined the phase and lattice parameter of the samples. The instrument characterized the phase with scan range of 10.00-80.00 degree.

Morphology and compositional purity have characterized by Scanning Electron Microscope (SEM) and Energy Dispersive X-Ray (EDX). Scanning Electron Microscope has characterized samples with the value voltage acceleration at 30.0 kV and 100 micrometers for zooming.

The magnetization of the samples has characterized by Vibrating Sample Magnetometer with the source magnetic field at 1 Tesla at room temperature.

3. RESULTS AND DISCUSSION

The XRD pattern of polycrystalline $La_{0.7}Ba_{0.21}Ca_{0.09}Mn_{1-x}Ni_xO_3$ shown in Figure 1. From the XRD pattern shown that the increase of Ni^{+3} ion on the samples were not changing the phase. Moreover the refinement result by HighScore Plus software shown that all samples have same crystalline structure and same space group which the crystalline structure is Rhombohedral and R-3c space group. The refinement result was listed in Table 1.

Table 1. Structure parameters of polycrystalline $La_{0.7}Ba_{0.21}Ca_{0.09}Mn_{1-x}Ni_xO_3$ (x = 0.1; 0.2; 0.3)

Parameter Structure	x = 0.1	x = 0.2	x = 0.3
Space group	R-3c	R-3c	R-3c
Crystal structure	Rhombohedral	Rhombohedral	Rhombohedral
a (Å)	5.514042	5.49198	5.48329
b (Å)	5.514042	5.49198	5.48329
c (Å)	13.5058	13.51009	13.51076
Volume ($Å^3$)	355.624	353.7581	351.797
<Mn-O> (Å)	1.953	1.95053	1.9469
<Mn-O-Mn> (°)	109.1	108.742	108.78

Crystaline Size (nm)	19.27	19.35	15.44
Distribution Particle Size (nm)	96-159	60-95	53-145
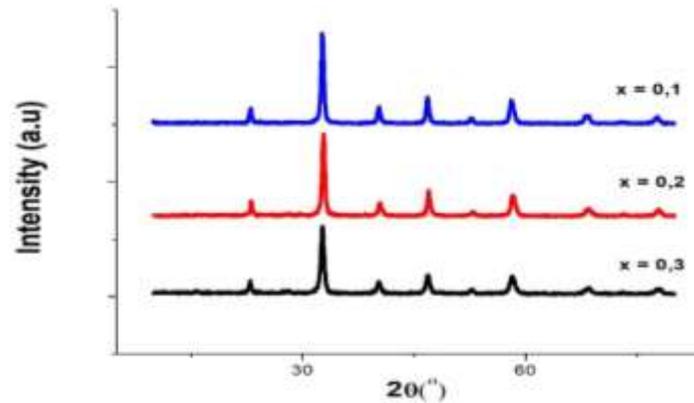
Figure 1. XRD pattern of polycrystalline $La_{0.7}Ba_{0.21}Ca_{0.09}Mn_{1-x}Ni_xO_3$ (x = 0.1; 0.2; 0.3)

Based on Table 1, the lattice parameter c was not changed significantly, but the lattice parameter a and b has decreased while the increasing of Ni^{+3} ion on the samples. The decreasing happened because the ionic radii Ni^{+3} is smaller than the ionic radii Mn^{+3} (Saptari, et al, 2017; Slater, 1964; Yadav, et al, 2016), and volume have decreased with the decreasing of lattice parameter a and b. The decreasing volume shown in Figure 2.
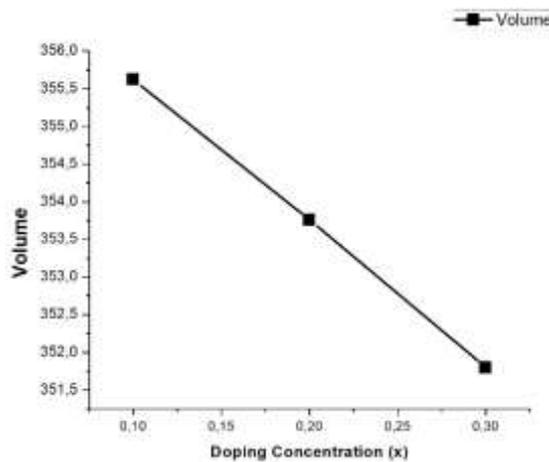
Figure 2. Graph between volume – doping concentration of $La_{0.7}Ba_{0.21}Ca_{0.09}Mn_{1-x}Ni_xO_3$
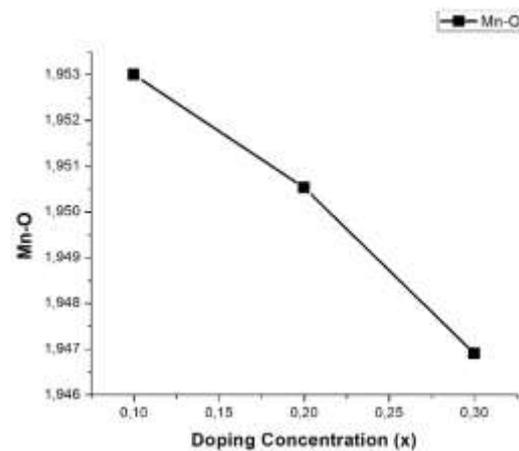
Figure 3. Graph between distance Mn-O – doping concentration of $La_{0.7}Ba_{0.21}Ca_{0.09}Mn_{1-x}Ni_xO_3$

The distance between Mn-O on $La_{0.7}Ba_{0.21}Ca_{0.09}Mn_{1-x}Ni_xO_3$ shown in Figure 3. The figure shown that the distance has decreased with the increasing substitution of Ni+3 ion, those things happened because when the sample has added by Ni^{+3} ion, the Mn^{+3} ion has replaced by Ni^{+3} ion. It might be the sample with composition x = 0.3 have lower currie temperature than other samples, because when the distance Mn-O went high, it would make the currie temperature higher than when the distance Mn-O went small (Zhang, et al, 2001).

The result of morphology and distribution particle size of the samples $La_{0.7}Ba_{0.21}Ca_{0.09}Mn_{1-x}Ni_xO$ from characterized by SEM shown in Figure 4. Those figure shown that all samples are homogeneity and have nanometer distribution particle size, that has explain in Table 1.

(a) (b) (c)
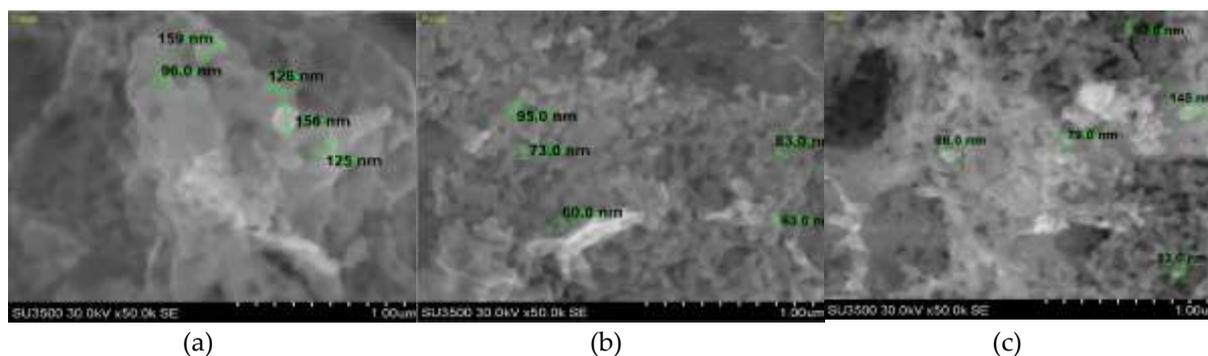
Figure 4. SEM images of polycrystaline $La_{0.7}Ba_{0.21}Ca_{0.09}Mn_{1-x}Ni_xO_3$, (a) 0.1; (b) 0.2; (c) 0.3

(a) (b) (c)
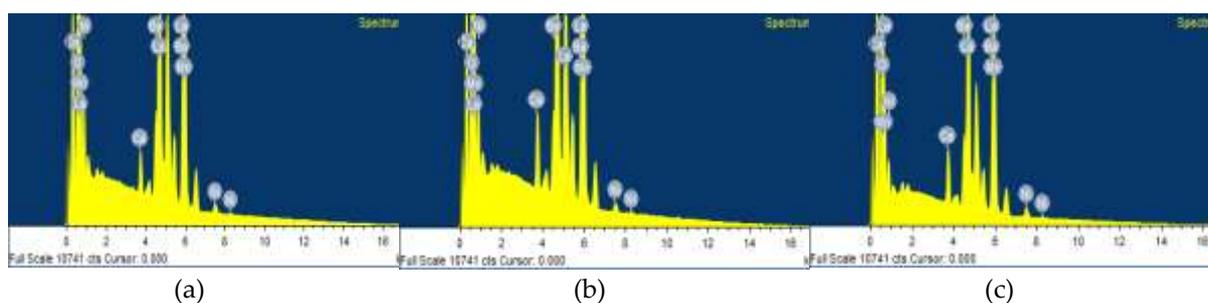
Figure 5. EDX result of polycrystaline $La_{0.7}Ba_{0.21}Ca_{0.09}Mn_{1-x}Ni_xO_3$, (a) 0.1; (b) 0.2; (c) 0.3

Table 2. Comparison at.% between sample composition (theory) and (real) of polycrystalline $La_{0.7}Ba_{0.21}Ca_{0.09}Mn_{1-x}Ni_xO_3$

Doping concentration	Element composition	Sample composition (theory) (at.%)	Sample composition (real) (at.%)
	La	14.00	10.28
	Ba	4.20	2.156
x = 0.1	Ca	1.80	0.844
	Mn	18.00	10.28
	Ni	2.00	0.512
	O	60.00	73.914
	La	14.00	10.816
	Ba	4.20	1.782
x = 0.2	Ca	1.80	1.408
	Mn	16.00	12.458
	Ni	4.00	0.416
	O	60.00	73.122
	La	14.00	10.166
	Ba	4.20	2.276
x = 0.3	Ca	1.8	1.66
	Mn	14.00	12.77
	Ni	6.00	0.91
	O	60.00	72.22

Table 3. Saturation value of polycrystalline $La_{0.7}Ba_{0.21}Ca_{0.09}Mn_{1-x}Ni_xO_3$

Doping Composition	Magnetic Saturation (emu/mg)
x = 0.1	5.78477
x = 0.2	5.13221
x = 0.3	2.67593

Figure 5 is the result of EDX analyzed. The identification by EDX analyzed is to confirm that the particles of precursors have distributed. The composition of all samples explained in Table 2. From the table, there have the differences between the composition in theory and the composition in real from EDX analyzed. Those differences are because EDX analyzed based on semi-qualitative calculate (Saptari, et al, 2017).

Hysteresis loop from VSM characterized shown in figure 6. The figure shown that the magnetization of polycrystalline $La_{0.7}Ba_{0.21}Ca_{0.09}Mn_{1-x}Ni_xO_3$ has decrease with the substituted Ni^{+3} ion which is marked by the decreasing of the magnetic saturation value, that has explain on Table 3 and samples are soft magnetic material. The decreasing of magnetization is because when the Ni^{+3} ion added into the sample, it would change the relation of double exchange Mn^{+3}-O^{-2}-Mn^{+4} became antiferromagnetic alignment Mn^{+4}-O^{-2}-Mn^{+4}, Mn^{+3}-O^{-2}-Mn^{+3}, Ni^{+3}-O^{-2}-Ni^{+3}, and when the concentration Ni^{+3} ion increase, the atom (Mn^{+3},Mn^{+4},Ni^{+3}) will surround the same kind. That caused the magnetization has decrease with the substituting Ni^{+3} ion on Mn^{+3} ion composition (Saptari, Manaf & Kurniawan, 2014; Yadav, et al, 2016).
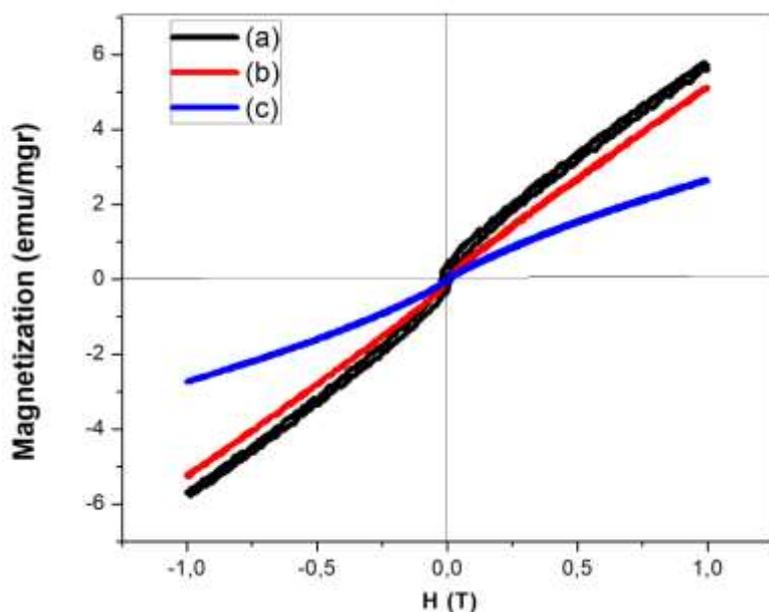
Figure 6. VSM pattern of polycrystalline $La_{0.7}Ba_{0.21}Ca_{0.09}Mn_{1-x}Ni_xO_3$, (a) 0.1; (b) 0.2; (c) 0.3

4. CONCLUSION

The synthesized of polycrystalline $La_{0.7}Ba_{0.21}Ca_{0.09}Mn_{1-x}Ni_xO_3$ (x = 0.1; 0.2; 0.3) by sol-gel method were successfully to make single phase with nanometer distribution particle size. Substitution Ni^{+3} ion does not influence to changing the phase significantly, all samples have rhombohedral crystal structure with space group R-3c, the lattice parameter a and b has decreased with increasing Ni^{+3} ion on the sample. The magnetization of samples has decreased with increasing substituting Ni^{+3} ion on the samples.

REFERENCES

Bhavani, A. G., Kim, W. Y. & Lee, J. S. (2013). Barium substituted lanthanum manganite perovskite for CO2 reforming of methane. *ACS Catal.*, 3(7), 1537–1544.

Cao, Y., Lin, B., Sun, Y., Yang, H. & Zhang, X. (2015). Synthesis, structure and electrochemical properties of lanthanum manganese nanofibers doped with Sr and Cu. *J. Alloys Compd.*, 638, 204–213.

Jiang, F., Zheng, J., Liang, L., Zhang, M. & Wang, Y. (2015). Microwave absorbing properties of La0.1Ca0.9MnO3porous microsphere synthesized by method of precipitation. *J. Mater. Sci. Mater. Electron.*, 26(4), 2243–2247.

Manjunatha, S. O., Rao, A., Lin, T. Y., Chang, C. M. & Kuo, Y. K. (2015). Effect of Ba substitution on structural, electrical and thermal properties of La0.65Ca0.35-xBaxMnO3(0 ≤ x ≤ 0.25) manganites. *J. Alloys Compd*., 619, 303–310.

McBride, K., Partridge, N., Bennington-Gray, S., Felton, S., Stella, L. & Poulidi, D. (2017). Synthesis, characterisation and study of magnetocaloric effects (enhanced and reduced) in manganate perovskites. *Mater. Res. Bull.*, 88, 69–77.

Millis, A.J. (1998). Lattice effects in magnetoresistive manganese perovskites. *Nature*, 392, 147–150.

Morelli, D. T., Mance, A. M., Mantese, J. V. & Micheli, A. L. (1996). Magnetocaloric properties of doped lanthanum manganite films. *J. Appl. Phys.*, 79(1), 373–375.

Nagabhushana, B. M., Sreekanth Chakradhar, R. P., Ramesh, K. P. , Prasad, V., Shivakumara, C. and Chandrappa, G. T. (2008). Magnetoresistance studies on barium doped nanocrystalline manganite. *J. Alloys Compd*., 450, 364–368.

Phan, M. H., Peng, H. X., Yu, S. C., Tho, N. D., Nhat, H. N. & Chau, N. (2007). Manganese perovskites for room temperature magnetic refrigeration applications. J. *Magn. Mater*., 316, 562–565.

Saptari, S., Manaf, A. & Kurniawan, B. (2014). Microwave Absorbing Properties Of La0.67 Ba0.33 Mn1-X NiX O3. *J. Sains Mater. Indonesia,* 15, Juli, 183–189.

Saptari, S. A., Tjahjono, A., Winarsih, S., Prasetyo, P. & Kurniawan, B. (2017). Effect of Ni-doping on Structure and Compounds by Sol-Gel Method. *Int. J. Basic Appl. Sci.*, 17(6), 12–16.

Sfifir, I., Ben Khlifa, H., Cheikhrouhou-Koubaa, W., Koubaa, M. & Cheikhrouhou, A. (2017). Vacancy effect in both calcium and barium on the physical properties of La0.6Ca0.2Ba0.2MnO3 polycrystalline manganite. *J. Alloys Compd.*, 693, 782–791.

Shankar, K. S. & Raychaudhuri, A. K. (2006). Low-temperature polymer precursor-based synthesis of nanocrystalline particles of lanthanum calcium manganese oxide (La0.67Ca0.33MnO3) with enhanced ferromagnetic transition temperature. J. Mater. Res., 21(1), 27–33.

Slater, J. C. (1964). Atomic radii in crystals. *J. Chem. Phys.*, 41(10), 3199–3204.

Stege, W. P., Cadús, L. E. & Barbero, B. P. (2011). La1-xCaxMnO3 perovskites as catalysts for total oxidation of volatile organic compounds. *Catal. Today*, 172(1), 53–57.

Xiong, Y. Q. et al., (2015). Electric field modification of magnetism in Au/La2/3Ba1/3MnO3/Pt device.

Yadav, A., Shah, J., Gupta, R., Shukla, A., Singh, S. & Kotnala, R. K. (2016). Role of spin-glass phase for magnetoresistance enhancement in nickel substituted lanthanum calcium manganite. *Ceram. Int.*, 42(11), 12630–12638.

Zhong, W., Chen, W., Au, C. T. & Du, Y. W. (2003). Dependence of the magnetocaloric effect on oxygen stoichiometry in polycrystalline La 2 / 3 Ba 1 / 3 MnO 3 – d. 261(1–2), 238–243.

Zhang, J., Tanaka, H., Kanki, T., Choi, J.-H. & Kawai, T. (2001). Strain effect and the phase diagram of La1ÀxBaxMnO3 thin films. *Phys. Rev. B*, 64(18), 184404..